

Flexible micromorph tandem a-Si/ μ c-Si solar cells

T. Söderström,^{a)} F.-J. Haug, V. Terrazzoni-Daudrix, and C. Ballif
Photovoltaics and Thin Film Electronics Laboratory, Institute of Microengineering (IMT), École Polytechnique Fédérale de Lausanne (EPFL), Rue A.-L. Breguet 2, CH-2000 Neuchâtel, Switzerland

(Received 2 October 2009; accepted 25 November 2009; published online 7 January 2010)

The deposition of a stack of amorphous (a-Si:H) and microcrystalline (μ c-Si:H) tandem thin film silicon solar cells (micromorph) requires at least twice the time used for a single junction a-Si:H cell. However, micromorph devices have a higher potential efficiency, thanks to the broader absorption spectrum of μ c-Si:H material. High efficiencies can only be achieved by mitigating the nanocracks in the μ c-Si:H cell and the light-induced degradation of the a-Si:H cell. As a result, μ c-Si:H cell has to grow on a smooth substrate with large periodicity ($>1 \mu\text{m}$) and the a-Si:H cell on sharp pyramids with smaller feature size ($\sim 350 \text{ nm}$) to strongly scatter the light in the weak absorption spectra of a-Si:H material. The asymmetric intermediate reflector introduced in this work uncouples the growth and light scattering issues of the tandem micromorph solar cells. The stabilized efficiency of the tandem n-i-p/n-i-p micromorph is increased by a relative 15% compared to a cell without AIR and 32% in relative compared to an a-Si:H single junction solar cells. The overall process ($T < 200 \text{ }^\circ\text{C}$) is kept compatible with low cost plastic substrates. The best stabilized efficiency of a cell deposited on polyethylene-naphthalate plastic substrate is 9.8% after 1000 h of light soaking at V_{oc} , 1 sun, and $50 \text{ }^\circ\text{C}$. © 2010 American Institute of Physics.
 [doi:10.1063/1.3275860]

I. INTRODUCTION

Solar energy conversion has the potential to satisfy the electricity and even the total energy consumption of the world. Indeed, 1 h of solar irradiation on Earth is equivalent to the total world energy consumption in 1 year. Photovoltaic (PV) or the direct conversion of sunlight into electricity is a promising technology which can be easily installed without affecting neither the landscape nor the natural environment if directly integrated into building. Strong effort has been made in the past decade to decrease the cost per watt peak of PV. Indeed, the standard crystalline silicon technology, which has a 90% market share, has decreased the cost by a factor of 20 in 30 years. Further cost reduction can be made by using thinner films which use less material and large area monolithic integration while keeping the advantages of silicon i.e., durability, abundancy, and nontoxicity.¹ This paper reports on the design of high efficiency thin film silicon solar cells with processes compatible with flexible low cost plastic substrates.

The micromorph tandem solar cell, composed of an amorphous (a-Si:H) top cell and a microcrystalline (μ c-Si:H) bottom cell, is one of the most promising multi-junction candidates for high stabilized efficiency thin film silicon solar cells.² Indeed, the combination of a high a-Si:H band gap (1.7 eV) and a low μ c-Si:H band gap (1.1 eV) creates an almost ideal tandem device.³

The challenge of this device is to achieve ideal short circuit current density (J_{sc}) matching between the two sub-cells because in multijunction solar cells, the J_{sc} is limited by the lowest J_{sc} of the subcells. In micromorph tandem cells where an amorphous cell is just stacked on top of microcryst-

talline cell, the light passes through the top cell only once; the weakly absorbed light will pass into the bottom cell and is eventually absorbed there. The light-induced degradation⁴ forbids the use of thick a-Si:H solar cells. Therefore, in tandem micromorph cells, the limitation in J_{sc} comes usually from the top cell.

One widely used solution in the superstrate configuration (p-i-n) is to introduce a thin intermediate reflector⁵ (IR) which enhances the J_{sc} of the top cell without the need of increasing its absorber layer thickness. The IR is usually a material with a refractive index lower than silicon (typically $1.5 < n_{\text{IR}} < 3$ compared to $n_{\text{Si}} \sim 4$) in order to have an index contrast that increases the reflection of the light at the Si/IR interface. The IR is usually a thin layer, between 50 and 150 nm, deposited *in situ*^{6,7} or *ex situ*.⁸ *In situ* silicon oxide intermediate reflector (SOIR),⁹ silicon nitride,¹⁰ or *ex situ* zinc oxide intermediate reflector¹¹ has been reported to be very effective and are already implemented in complete products.¹² In the substrate configuration (n-i-p), the problem of obtaining high efficiency micromorph tandems with elevated stabilized J_{sc} in the top cell was not yet solved. So far, the alternative solution to avoid the problem of current matching is to implement triple junction solar cells which split the J_{sc} into the three subcells and therefore allow the use of thin a-Si:H top cells.¹³ Nonetheless, this strategy demands the implementation of a more complex process, e.g., one more cell and profiling^{14,15} of Ge in the a-Si:Ge solar middle cells.

In this paper, we first present the limitation of increasing the efficiency with a single junction a-Si:H [Fig. 1(a)] and μ c-Si:H [Fig. 1(b)] while increasing, respectively, the absorber thickness. Then, we concentrate our study on the J_{sc} limitation for tandem micromorph cell in the initial and stabilized state without IR [Fig. 1(c)] and with IR [Fig. 1(d)].

^{a)}Electronic mail: thomas.soderstrom@epfl.ch.

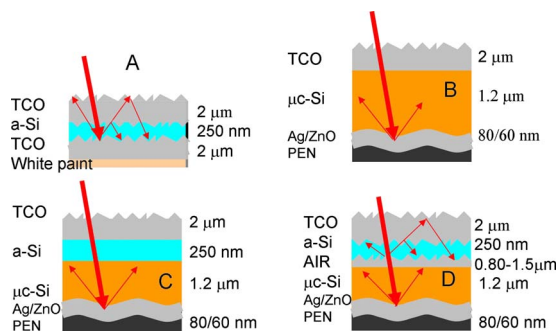


FIG. 1. (Color online) (a) Schema of single junction a-Si:H, (b) single junction $\mu\text{c-Si:H}$, (c) tandem micromorph a-Si:H/ $\mu\text{c-Si:H}$, and (d) tandem micromorph with AIR deposited on textured substrates covered with thin Ag/ZnO.

We have shown in a previous study¹⁶ that a thin IR increases the J_{sc} of the top cell but more important that the implementation of an asymmetric intermediate reflector (AIR) is much more effective for n-i-p/n-i-p tandem micromorph solar cells. Therefore, we investigate the potential gain in J_{sc} of the a-Si:H top cell in the initial and stable state with an AIR. Finally, we present the best results obtain on glass and on plastic substrate with 10.1% and 9.8% stable efficiencies, respectively.

II. EXPERIMENTAL

The absorber layer of a-Si:H and $\mu\text{c-Si:H}$ are deposited by very high frequency plasma enhanced chemical vapor deposition in a small area deposition chamber (substrate size of $8 \times 8 \text{ cm}^2$). The temperature is kept below $200 \text{ }^\circ\text{C}$ to be compatible with flexible low T_g plastic substrates.

We use three types of substrate; the first one consists of silver¹⁷ deposited by sputtering onto heated glass substrates, and then covered with 60 nm ZnO for optical matching.¹⁸ The typical root mean square (rms) roughness of this “hot silver” substrate is between 40 and 60 nm. The second type of substrate consists of ZnO deposited by low pressure chemical vapor deposition (LP-CVD).¹⁹ The rms roughness of this substrate is typically between 60 and 70 nm for a $2 \text{ }\mu\text{m}$ thick film. Finally, the third type of substrate is fully flexible plastic substrate [polyethylene-naphthalate (PEN)] whose surface consists of a two-dimensional (2D) sinusoidal grating with a rms roughness of 70 nm, covered with a thin nominally flat double layer of 80 nm silver and 60 nm ZnO.²⁰ The rigid substrates are used for reference and development, but all process steps are kept compatible with the plastic substrate, i.e., $T < 200 \text{ }^\circ\text{C}$.

The front transparent conductive oxide (TCO) consists of boron doped ZnO deposited by LP-CVD. The AIR is also ZnO deposited by LP-CVD but without adding dopant during the deposition. This reduces the absorption losses by free carriers in this nonactive layer without any additional cost because high lateral conductivity is not beneficial for AIR.

The current-voltage (IV) measurement is performed with a class A dual lamp (Wacom) simulator. From this measurement, V_{oc} and fill factor (FF) are obtained. The J_{sc} is calculated from the external quantum efficiency measurement calibrated with a c-Si photodiode. The IV curve is, then,

normalized with this J_{sc} . This conservative method avoids any uncertainties on the surface area of the solar cells. The cell area is between 0.3 and 0.5 cm^2 .

Cross-sectional analysis is carried out by focused ion beam milling in a scanning electron microscope (SEM) by D. Alexander at the Interdisciplinary Centre for Electron Microscopy (CIM) in the EPFL.

The stabilization procedure applied to both a-Si:H and micromorph tandem cells exposes the solar cells to 1000 h light soaking at $50 \text{ }^\circ\text{C}$, 50 mW/cm^2 , and V_{oc} condition. Note that the record cell on plastic foil has been subjected to a more severe light soak of 100 mW/cm^2 .

III. RESULTS

A. Amorphous solar cells

The light-induced degradation of amorphous material is the issue that is the most critical to mitigate in the solar cell. This effect was first evidenced by Staebler and Wronski in 1977.⁴ Furthermore, Yang *et al.*²¹ and Hata *et al.*²² reported that the long term stability is governed by the competition between light-induced degradation and thermal annealing. Hence, a steady state also called “stabilized state” can be reached, typically after 1000 h under light soaking condition.

In a-Si:H silicon solar cells, the degradation depends mostly on the thickness of the absorber layer.^{23,24} In fact, a thinner cell has a higher electric field in the absorber layer, hence a higher collection efficiency of the photogenerated charged carriers. Therefore, the recombination process within the absorber is reduced. It was reported by Benagli *et al.*²⁴⁻²⁶ that the cell efficiency degradation depends on the absorber thickness but also on the buffer layer (close to the p-side) thickness and the substrate morphology for p-i-n a-Si:H solar cells. In Fig. 2, the effect of the absorber layer thickness is also shown in our n-i-p a-Si:H solar cell deposited on textured LP-CVD ZnO substrate even with our rather low process temperature ($< 200 \text{ }^\circ\text{C}$). The structure of the cell glass/LP-CVD ZnO/a-Si/LP-CVD ZnO was presented elsewhere.²⁷ Note that in our series, the solar cells do not have any buffer layer close to the p-side nor on the n-side. The degradation of the n-i-p a-Si:H is decreased from 27% to 10% when the absorber thickness is decreased from 400 to 140 nm and the optimum cell thickness is around 200 nm in the stable state. The cell with a 140 nm thick layer loses in V_{oc} and this is mostly due to the appearance of shunts in the thin device, possibly growth-induced cracks on severely textured LP-CVD ZnO substrates.²⁸ Note that in our cells, the J_{sc} and FF are the parameters that degrade the most significantly. In our case, the cells degrade mostly in J_{sc} by 1 mA/cm^2 and in FF by 10%.

B. Microcrystalline ($\mu\text{c-Si:H}$) solar cells

For high efficiency multijunction devices, a maximum of light absorption is required in the infrared wavelengths. With fixed material properties, we work on two ways to increase the absorption in the solar cell. First, we implement light trapping technique by including a 2D periodic substrate as already presented elsewhere.^{20,29} Second, we increase the thickness of the $\mu\text{c-Si:H}$ bottom cells. Here, we illustrate

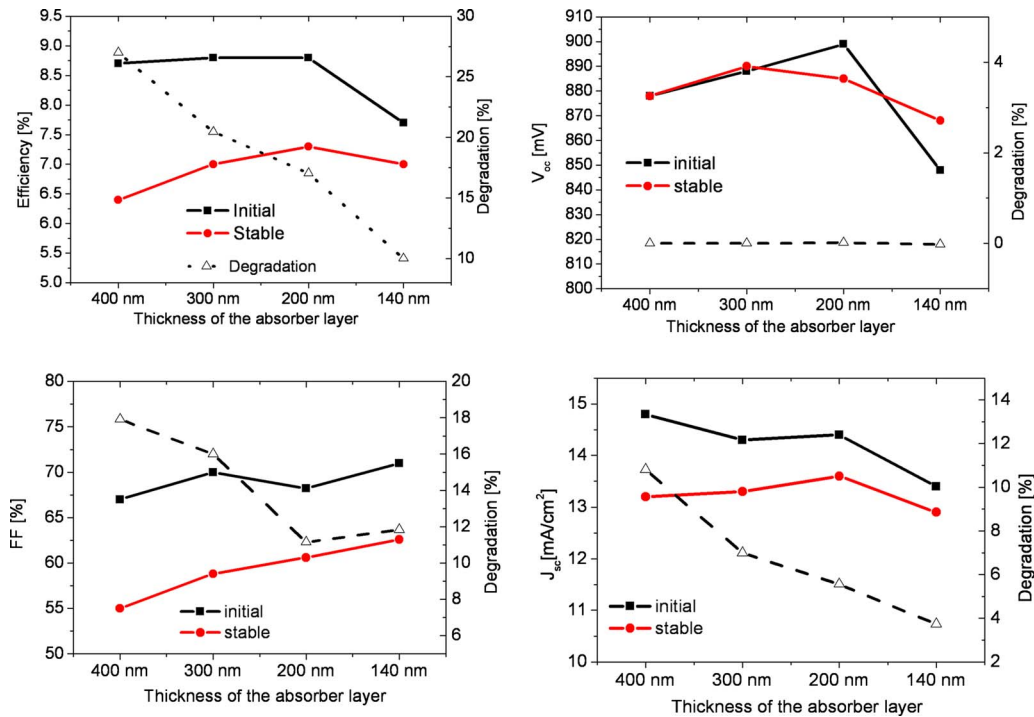


FIG. 2. (Color online) Initial (squares) and stable (circles) parameters for various thicknesses of a-Si:H absorber layer. The cells are deposited on glass coated with LP-CVD ZnO and surface plasma treated for 6 min (Ref. 27). The triangles show the relative degradation of the cell on the right axis.

this effect with a thickness series of $\mu\text{c-Si:H}$ solar cells, as shown in Table I and Fig. 3. The J_{sc} increases from 22.9 to 25.1 mA/cm^2 with increasing thickness of the absorber layer from 1 to 3 μm . The V_{oc} and FF are, here, only moderately reduced by the increase in the thickness to 2.5 μm . In this series an efficiency of 8.8% on plastic substrates has been obtained. Note that with 3 μm thick absorber layer, the J_{sc} is only slightly increased compared to 2.5 μm . In fact, a thickness of the cell over 2.5 μm starts to cause deleterious carrier collection problems as also reported elsewhere³⁰ and shown by the reduced V_{oc} and FF for the 3 μm thick $\mu\text{c-Si:H}$ solar cell in Table I. We note this effect for solar cells deposited on hot silver as well. Nevertheless, this effect can be mitigated as reported by Sai and Kondo.³¹

C. Micromorph n-i-p tandem cells without IRs

Here, we present the results of micromorph tandem cells without an IR between the top and bottom cells, as shown in Fig. 1(c). The substrate is the hot silver deposited on glass. Then, the $\mu\text{c-Si:H}$ cell is deposited. The surface of the $\mu\text{c-Si:H}$ cell acts as textured “substrate” for the a-Si:H top

TABLE I. Electrical parameters of $\mu\text{c-Si:H}$ solar cells on 2D grating with thicknesses of the absorber layer varying from 1 to 3 μm .

Thickness	V_{oc} (mV)	FF (%)	J_{sc} (mA/cm^2)	Efficiency (%)
1.1	513	69	22.9	8.1
1.5	528	69	24.2	8.8
2	517	67	24.5	8.4
2.5	515	67	25.0	8.6
3	488	60	25.1	7.3

cell. It was previously shown²⁹ that the growth of the $\mu\text{c-Si:H}$ absorber reduces the texture of the substrate which consequently reduces the possibility of light scattering in the top cell. The light-induced degradation of a micromorph tandem cell is mainly driven by the increase in defect density in the a-Si:H material. Indeed, there is an optimum between the reduction in the top cell thickness and the light-induced degradation of the tandem, which partly is driven by the decrease in J_{sc} of the a-Si:H cell, as shown in Table II. It shows, as expected, that the thicker the a-Si:H absorber, the higher the degradation of the micromorph cells; it is almost 20% for thick (300–600 nm) a-Si:H absorber and only 13% for 160 nm thick a-Si:H absorber.

Our tandem solar cells degrade mostly in J_{sc} and FF, similar to the single a-Si:H junction case. Note that FF can be strongly affected by the current density matching of the two subcells.^{32,33} Therefore, we concentrate our study on the light-induced degradation of the J_{sc} of the top cell. Figure 4 shows the initial and stabilized J_{sc} versus the a-Si:H top cell

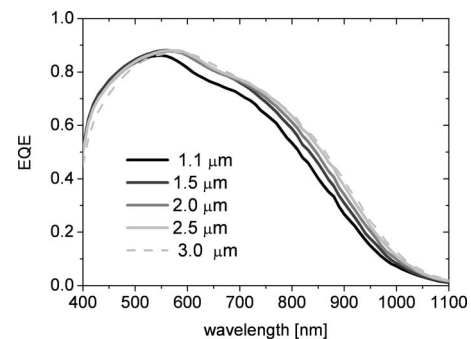


FIG. 3. EQE of a $\mu\text{c-Si:H}$ solar cell with absorber thickness increasing from 1 to 2.5 μm .

TABLE II. Initial and stable (in parentheses) parameters of the n-i-p micromorph tandem solar cells with various thicknesses of the a-Si:H top cell. The substrates for these micromorph cells are hot silver.

a-Si:H (nm)	V_{oc} (V)	FF (%)	J_{top} (mA/cm ²)	J_{bottom} (mA/cm ²)	Eff. (%)	Deg. (%)
160	1.36(1.36)	77(70)	9.1(8.7)	12.9(12.5)	9.6(8.3)	13
220	1.27(1.25)	74(66)	9.5(8.9)	14.9(14.6)	8.9(7.4)	16
300	1.35(1.34)	73 (62)	10.7(10.3)	11.5(11.2)	10.5(8.6)	18
400	1.33(1.32)	65 (59)	11.8(10.6)	13.8(13.3)	10.2(8.3)	19
600	1.25(1.26)	58 (53)	12.1(9.9)	11.3(11.1)	8.2(6.6)	19

thicknesses of micromorph tandem cells deposited on hot silver substrates. The initial J_{sc} saturates at 12 mA/cm² whereas the stable J_{sc} saturates at about 10.5 mA/cm². This clearly limits the efficiency of the tandem device since the current density of 25 mA/cm² in the microcrystalline device of Sec. III B would allow a potential matched current density of 12.5 mA/cm². Therefore, the simple tandem device optical design without IR clearly limits the cell performances to 10% in the stabilized state assuming the best J_{sc} of 10.5 mA/cm² and optimistic $V_{oc}=1.4$ V and FF=70%. Note that for a tandem micromorph cell, the optimum a-Si:H top cell thickness for J_{sc} in the stable state is close to 400 nm. This thickness is thicker than our optimum thickness (200 nm) found for single junction solar cells prepared in Sec. III A and therefore, this also limits the potential FF of the tandem cell.

D. Micromorph tandems with IR

The mitigation of poor top cell current density is usually achieved by introducing an IR between the a-Si:H and the μc -Si:H cells. First, we include a thin IR consisting of SOIR as described by Buehlmann.⁶ Because of the reduced refractive index compared to silicon, the SiOx layer reflects part of the incoming light back into the top cell. However, the thin (100 nm) SiOx layer reproduces the surface texture of the bottom cell which is governed by the large feature size of the back reflector. This is clearly not an ideal situation for the amorphous cell because the back reflector texture has been designed for scattering of long wavelengths.

The J_{top} gain can be strongly enhanced with an AIR, which reflects, but also scatters the light into the top cell. We realize this concept by an IR layer of LPCVD-ZnO, as

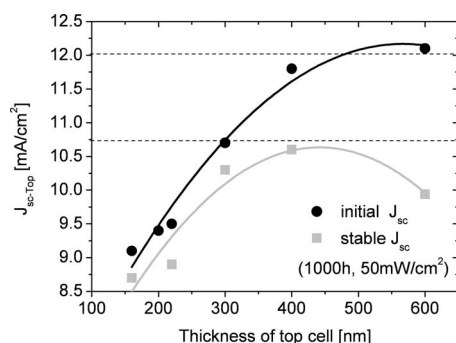


FIG. 4. Initial and stable top cell J_{sc} for various a-Si:H top cell absorber thicknesses deposited on hot silver substrates. The solid lines are guides for the eyes.

shown in Fig. 1(d). With this AIR, we obtain an efficient light incoupling in the top cell between the AIR and the front contact. In fact, the roughness of the AIR is carried through the top cell thickness, resulting in light scattering at both the front and the back interface of the a-Si:H top cell. Thus, our AIR consisting of thick textured ZnO deposited by LP-CVD introduces light scattering in addition to reflection at the index contrast, which underlies the simple conformal IR.

Figure 5 presents a SEM cross-section view of the structure of the device with AIR. The substrate consists of a PEN foil with the 2D grating and covered with a thin Ag/ZnO, which is used as a back contact and a back reflector. Then, 2.8 μm of μc -Si:H is deposited as a bottom cell, 1.5 μm of LP-CVD ZnO as AIR, 180 nm of a-Si:H as a top cell, and finally 4 μm of ZnO LP-CVD as a front contact. The structure is designed with the aim of having soft or U-shape morphology texture, which preserves the quality of the μc -Si:H material and still has elevated scattering of the red light, between 800 and 1000 nm. This is the reason why the feature size is kept large (1.2 μm) and the shape of the morphology is soft, i.e., no incised valleys. Then, the AIR serves as optimum AIR with sharp textured morphology and feature sizes of 300 nm, which scatter efficiently the blue-green light in the a-Si:H top cell.

The effects of the IRs are shown in Fig. 6, where the EQE of three top a-Si:H cells of n-i-p micromorph tandem solar cells, without IR, with 100 nm thin SOIR IR with ($n_{SOIR}=2$ at 600 nm) and with AIR of 1.5 μm of LP-CVD ($n_{AIR}=1.8$ at 600 nm), are compared. All a-Si:H top cells have equal absorber thicknesses of 200 nm. The J_{sc} of the top cell increases with the introduction of the IR. In Fig. 6, the thin IR increases the J_{sc} by an absolute 0.7 mA/cm², whereas the AIR increases the J_{sc} by 3 mA/cm². At 650 nm, the relative gain in the EQE is 60% for the thin IR and 220% for the AIR. We attribute the effect of the AIR mainly to its

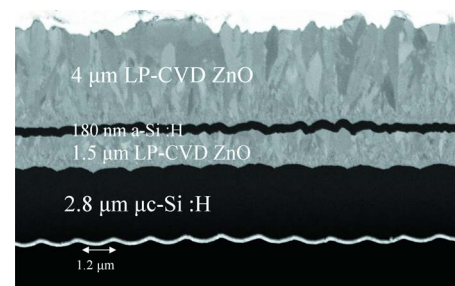


FIG. 5. (Color online) SEM micrographs of a cross-section of a n-i-p micromorph with AIR deposited on plastic foils (PEN).

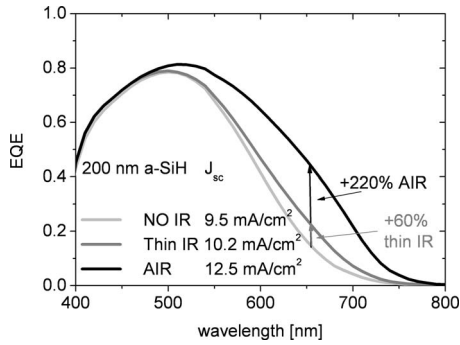


FIG. 6. EQE of 200 nm top a-Si:H in n-i-p micromorph solar cell without IR, with a thin IR (silicon oxide IR), and with AIR (1.5 μm thick LP-CVD ZnO).

texture; indeed, the $\mu\text{c-Si:H}$ layer even smoothes the initial substrate texture but the AIR establishes a roughness, which creates ideal light scattering for the top cell. Therefore, the light is both reflected and scattered by the AIR. This creates light trapping in the a-Si:H top cell, sandwiched between the top front contact and the IR.

E. Reflection losses due to the IRs

The IRs enhance the J_{sc} of the top cell but part of the weakly absorbed light is also outcoupled from the solar cell due to reflection at the IR. Figure 7 shows the typical total reflection curves obtained with thin IR, with AIR and without IR. The reflection curve of the cell with a thin IR shows an interference that comes from the flat or almost flat interfaces after the $\mu\text{c-Si:H}$ deposition. For the AIR case, the interference disappears due to the light scattering. The roughness of the AIR decreases slightly the primary reflection (about 1%) between 400 and 600 nm, thanks to the higher roughness at the Si/TCO interface, which provides a refractive index gradient, slightly reducing the reflection at the front Si/TCO interface. From 830 to 950, the reflection is higher with the thin IR compared to the AIR. The interference effect of the thin IR can be tuned to be varied in wavelength, whereas with the AIR the effect is more constant.

Figure 8 shows the EQE comparison of two micromorph cells, one with a 610 nm thick a-Si:H top cell and the second with a 200 nm thick a-Si:H top cell combined with an AIR. For both cells, the bottom cells have equal thicknesses. The J_{sc} of the a-Si:H are equal (12.1 and 12.2 A/cm^2) even

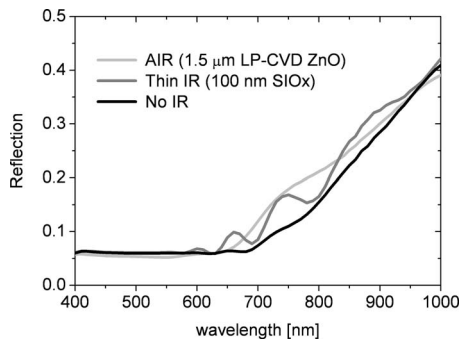


FIG. 7. Reflection curves of micromorph tandem cells without IR (light gray), with thin IR (gray), and with AIR (black)

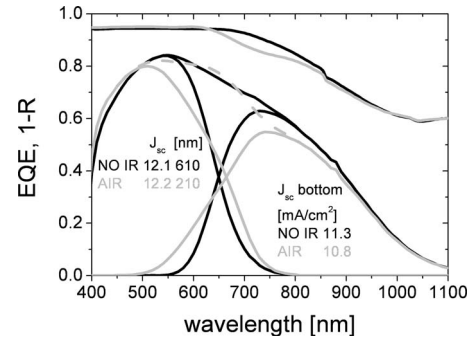


FIG. 8. EQE and 1-R of micromorph tandem cell without IR (black) and with AIR (gray). The top cell with AIR has an absorber thickness of 210 nm and the top cell without IR has an absorber thickness of 610 nm.

though the cell without AIR is three times thicker. Furthermore, for light wavelengths between 600 and 750 nm, the EQE of the cell with AIR is higher and thus the effective thickness is, in fact, higher than 3. The photogeneration distribution is different between the two structures. In fact, the cell without IR has higher EQE between 500 and 600 nm, whereas the EQE is higher from 600 to 750 nm for the cell with the AIR. The secondary reflection from the micromorph tandem cell with AIR increases between 550 and 900 nm for the cell. By integrating the differences in reflection, we estimated the potential losses around 0.4 mA/cm^2 . This potential loss corresponds to the loss observed in the total current density but this reflection loss is also combined with additional losses such as absorption in nonphotoactive layers, e.g., in the AIR (1.5 μm thick ZnO LP-CVD) due to defects and free carrier absorption, and absorption in the doped layers of the a-Si:H due to the multiplication light passes in the a-Si:H top cell. Nevertheless, these losses can be minimized by reducing the thickness of the doped layers and by using undoped (nonintentionally doped) LP-CVD ZnO. Indeed, in Fig. 9, we compare the total J_{sc} of a micromorph tandem cell with 1.5 μm undoped LP-CVD ZnO between the a-Si:H and the 3 μm $\mu\text{c-Si:H}$ cells with the J_{sc} of a single junction $\mu\text{c-Si:H}$ cell with 3 μm thick absorber layer. It shows that both totals J_{sc} are equal to 25.1 mA/cm^2 . The losses have not disappeared but the reflection losses are small (between 1% and 2% of the total J_{sc} only) and the absorption losses in nonactive layers are minimized.

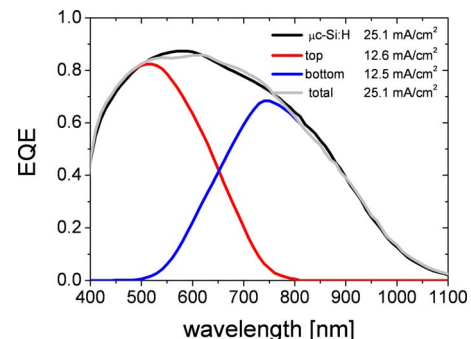


FIG. 9. (Color online) EQE of $\mu\text{c-Si:H}$ cell with 3 μm thick absorber layer and EQE of micromorph tandem cell with an AIR of 1.5 μm ZnO LP-CVD and a 3 μm thick bottom cell deposited on the 2D cross grating.

TABLE III. Performance parameters of the micromorph tandem solar cells deposited on hot silver without IR and with AIR. The stabilized parameters are given in parentheses and the relative degradation (Deg.) is given in the last column.

Thickness a-Si/ μ m-Si (μ m)	V_{oc} (mV)	FF (%)	J_{top} (mA/cm ²)	J_{bottom} (mA/cm ²)	Efficiency (%)	Deg. (%)
0.3/1.2 no IR	1.35(1.34)	73 (62)	10.7(10.3)	11.5(11.2)	10.5(8.6)	18
0.14/1.4 AIR	1.32(1.34)	74 (70)	11.4(10.3)	10.6(10.2)	10.4(9.6)	8
0.18/3 AIR	1.32(1.35)	66 (65)	12.4(11.7)	11.9(11.5)	10.3(10.1)	3

F. Solar cell efficiency and degradation with AIR

The AIR increases the effective thickness of the a-Si:H layer, which is crucial for limiting the light-induced degradation of the micromorph tandem cell. In Table III, we compare the typical degradation for micromorph cells without IR and with AIR. The degradation is between 15% and 20% for a top cell of 300 nm without IR, whereas the degradation is limited to 0%–10% for the a-Si:H cell thickness below 200 nm and an AIR. The results shown in Table III are obtained on glass covered with hot silver and a LP-CVD ZnO front contact. The results obtained with AIR in Table III have a stable efficiency of 9.6% with 1.4 μ m thick μ c-Si:H bottom cells and 10.1% with 3 μ m thick bottom cells with only 8% and 3% relative degradation, respectively.

We deposit micromorph tandem cells with different a-Si:H cell thicknesses with and without AIR and evaluate the light-induced degradation. Again, we discard bias in FF due to different matching conditions and we concentrate on the light-induced degradation of the a-Si:H top cell J_{sc} . Figure 10 compares the J_{sc} of micromorph tandem cells with and without AIR. It shows that in the initial state, the AIR can provide J_{sc} up to 14 mA/cm² for a 300 nm thick a-Si:H top cell, whereas a cell without IR can hardly reach more than 12 mA/cm². In the stable state, the situation is even more critical because the J_{sc} with the AIR attains more than 12 mA/cm² with only 200 nm, whereas only 10.5 mA/cm² is achieved without IR and thicker amorphous absorber. The relative efficiency gain is close to 15%, thanks to the J_{sc} . In addition, not only the J_{sc} but also the FF in stabilized state should be improved if we transfer the results from the single junction a-Si:H thickness series of Fig. 2. Our experimental results of Table III confirm the efficiency gains in the stabilized state with the AIR. The best stable efficiency on glass

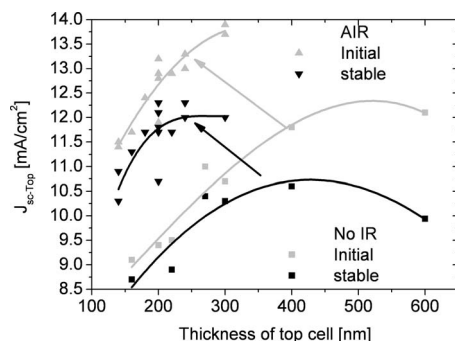


FIG. 10. Top cell J_{sc} of initial and stable (1000 h, 50 °C, and 50 mW/cm²) micromorph tandem cells with and without AIR. The solid lines are guides for the eyes.

covered with hot silver substrate and on flexible substrate are 10.1% and 9.8%, respectively. The cell on plastic substrate has an initial efficiency of 11.2% and was previously presented in Ref. 16.

IV. DISCUSSION

The single junction solar cells have initial efficiency close to 9% for both a-Si:H and μ c-Si:H solar cells. Our results show that going to the tandem micromorph structure improves the initial efficiency to more than 11%. Clearly, the increase in light absorption with the combination of two different band gaps and the implementation of the AIR is the key to this improvement.

So far, the best design for n-i-p solar cell is a triple junction device as used by Unisolar.³⁴ One advantage of the triple junction structure is the reduced degradation of the top cell since it can be made thinner than in a high efficiency tandem cell. The AIR concept is an alternative solution to combine thin amorphous cell, high efficiency tandem cells, and by using neither the triple junction devices nor germanium. The drawback of the micromorph concept with IR compared to the triple junction are reflection losses which, as shown in this work, can be reduced below 2% in relative, and it is in compensation for the reduced degradation of the micromorph tandem device. The best triple junction devices with Ge degrades by only 10%,³⁴ which is comparable to degradation obtained here for a n-i-p micromorph tandem cell, as shown in Table III.

In summary, we have fully implemented an AIR that selectively scatters the blue-green light into the top cell whereas the scattering of the red light into the bottom cell is achieved by the back reflector structure which is applied to the substrate. Such a structure can reach matched J_{sc} over 12 mA/cm² in the stabilized state, which is a necessary starting point for realizing 12% stable efficiencies in micromorph tandem cells on plastic substrates (assuming, e.g., a V_{oc} of 1.4 V and a FF of 71%). Note that stable J_{sc} of 12 mA/cm² corresponds to state-of-the-art micromorph tandem cells reported by Unisolar³⁴ and Kaneka³⁵ (assuming four segments in Ref. 35).

V. CONCLUSION

The combination of the high energy band gap (1.7 eV for a-Si:H) and low energy band gap (1.1 eV μ c-Si:H) in the micromorph tandem cell is almost ideal. Nonetheless, many technical constraints have to be taken into account to achieve high conversion efficiency cells and this is especially true for

n-i-p solar cells. In order to keep the light-induced degradation at a low level in the micromorph n-i-p/n-i-p tandem solar cell, the AIR concept is required because the deposition of the $\mu\text{c-Si:H}$ deposition flattens the initial large feature size textured surface of the substrate adapted for the light scattering of the bottom cell. Therefore, the AIR restores the ideal small feature size texture for the a-Si:H solar cell. It reflects the green light but also it scatters the light which creates an ideal coupling of the green light in the a-Si:H top cell. By including this tool in our device, we were able to fabricate a micromorph tandem cell with close to 10% stabilized efficiency on glass and plastic substrate.

- ¹M. A. Green, *Prog. Photovoltaics* **17**, 183 (2009).
- ²J. Meier, S. Dubail, S. Golay, U. Kroll, S. Fay, E. Vallat-Sauvain, L. Feitknecht, J. Dubail, and A. Shah, *Sol. Energy Mater. Sol. Cells* **74**, 457 (2002).
- ³F. Meillaud, A. Shah, C. Droz, E. Vallat-Sauvain, and C. Miazza, *Sol. Energy Mater. Sol. Cells* **90**, 2952 (2006).
- ⁴D. L. Staebler and C. R. Wronski, *Appl. Phys. Lett.* **31**, 292 (1977).
- ⁵D. Fischer, S. Dubail, J. A. A. Selvan, N. P. Vaucher, R. Platz, C. Hof, U. Kroll, J. Meier, P. Torres, H. Keppner, N. Wyrsh, M. Goetz, A. Shah, and K.-D. Ufert, Proceedings of the 25th IEEE PVSC, 1996 (unpublished), pp. 1053–1056.
- ⁶P. Buehlmann, J. Bailat, D. Domine, A. Billet, F. Meillaud, A. Feltrin, and C. Ballif, *Appl. Phys. Lett.* **91**, 143505 (2007).
- ⁷K. Yamamoto, A. Nakajima, M. Yoshimi, T. Sawada, S. Fukuda, T. Suezaki, M. Ichikawa, Y. Koi, M. Goto, and T. Meguro, *Prog. Photovoltaics* **13**, 489 (2005).
- ⁸D. Domine, J. Bailat, J. Steinhauser, A. Shah, and C. Ballif, Proceedings of the Fourth World Conference on Photovoltaic Energy Conversion, 2006 (unpublished).
- ⁹D. Dominé, P. Buehlmann, J. Bailat, A. Billet, A. Feltrin, and C. Ballif, *Phys. Status Solidi (RRL)* **2**, 163 (2008).
- ¹⁰P. Vineri, L. Mercaldo, I. Usatii, P. Ciani, and C. Privato, Proceedings of the 23rd European PVSEC, 2006 (unpublished).
- ¹¹D. Dominé, J. Bailat, J. Steinhauser, A. Shah, and C. Ballif, Proceedings of the Fourth World WCPEC, 2006 (unpublished), pp. 1465–1468.
- ¹²K. Yamamoto, A. Nakajima, M. Yoshimi, T. Sawada, S. Fukuda, T. Suezaki, M. Ichikawa, Y. Koi, M. Goto, T. Meguro, T. Matsuda, M. Kondo, T. Sasaki, and Y. Tawada, *Sol. Energy* **77**, 939 (2004).
- ¹³J. Yang, A. Banerjee, and S. Guha, *Appl. Phys. Lett.* **70**, 2975 (1997).
- ¹⁴J. Zimmer, H. Stiebig, and H. Wagner, *J. Appl. Phys.* **84**, 611 (1998).
- ¹⁵S. Guha, J. Yang, A. Pawlikiewicz, T. Glatfelter, R. Ross, and S. R. Ovshinsky, *Appl. Phys. Lett.* **54**, 2330 (1989).
- ¹⁶T. Söderström, F.-J. Haug, X. Niquille, V. Terrazzoni, and C. Ballif, *Appl. Phys. Lett.* **94**, 063501 (2009).
- ¹⁷R. H. Franken, R. L. Stolk, H. Li, C. H. M. d. Werf, J. K. Rath, and R. E. I. Schropp, *J. Appl. Phys.* **102**, 014503 (2007).
- ¹⁸A. Banerjee and S. Guha, *J. Appl. Phys.* **69**, 1030 (1991).
- ¹⁹J. Steinhauser, S. Fay, N. Oliveira, E. Vallat-Sauvain, and C. Ballif, *Appl. Phys. Lett.* **90**, 142107 (2007).
- ²⁰F. J. Haug, T. Söderström, M. Python, V. Terrazzoni-Daudrix, X. Niquille, and C. Ballif, *Sol. Energy Mater. Sol. Cells* **93**, 884 (2009).
- ²¹L. Yang, L. Chen, and A. Catalano, *Appl. Phys. Lett.* **59**, 840 (1991).
- ²²N. Hata and S. Wagner, *J. Appl. Phys.* **72**, 2857 (1992).
- ²³M. S. Bennett, J. L. Newton, and K. Rajan, Seventh EPVSEC, 1986 (unpublished), p. 544.
- ²⁴S. Benagli, U. Kroll, J. Meier, D. Borrello, and J. Spitznagel, Proceedings of the 23rd EUPVSEC, Milan, Italy, 2007 (unpublished).
- ²⁵S. Benagli, U. Kroll, J. Meier, D. Borrello, J. Spitznagel, G. Androuso-poulos, G. Monteduro, D. Zimin, O. Kluth, T. Roschek, C. Ellert, W. Stein, G. Buechel, A. Buechel, and D. Koch-Ospelt, Proceedings of the 21st EUPVSEC, Dresden, Germany, 2006 (unpublished), p. 1719.
- ²⁶S. Benagli, J. Hoetzel, D. Borrello, J. Spitznagel, U. Kroll, J. Meier, E. Vallat-Sauvain, J. Bailat, L. Castens, P. Madliger, B. Dehbozorgi, G. Monteduro, M. Marmelo, and Y. Djeridane, Proceedings of the 24th EUPVSEC, Valencia, Spain, 2008 (unpublished).
- ²⁷T. Söderström, F. J. Haug, V. Terrazzoni-Daudrix, and C. Ballif, *J. Appl. Phys.* **103**, 114509 (2008).
- ²⁸H. Sakai, T. Yoshida, T. Hama, and Y. Ichikawa, *Jpn. J. Appl. Phys., Part 1* **29**, 630 (1990).
- ²⁹T. Söderström, F. J. Haug, X. Niquille, and C. Ballif, *Prog. Photovoltaics* **17**, 165 (2009).
- ³⁰B. Schroeder, *Thin Solid Films* **430**, 1 (2003).
- ³¹H. Sai and M. Kondo, *J. Appl. Phys.* **105**, 094511 (2009).
- ³²D. Dominé, Ph.D. thesis, University of Neuchâtel, 2009.
- ³³A. Nakajima, M. Ichikawa, T. Sawada, M. Yoshimi, S. Fukuda, Y. Tawada, T. Meguro, H. Takata, T. Suezaki, and M. Goto, Proceedings of the Third World Conference PVSEC, 2003 (unpublished), pp. 1915–1918.
- ³⁴B. Yan, G. Yue, and S. Guha, *Mater. Res. Soc. Symp. Proc.* **989**, 335 (2007).
- ³⁵M. Green, K. Emery, D. King, Y. Hisikawa, and W. Warta, *Prog. Photovoltaics* **14**, 45 (2006).